



SPE 56539

A Laboratory Study on Oilwell Cement and Electrical Conductivity

K.R. Backe, S.K. Lyomov,* SPE, and O.B. Lile, SPE, Norwegian University of Science and Technology

Copyright 1999, Society of Petroleum Engineers Inc.

This paper was prepared for presentation at the 1999 SPE Annual Technical Conference and Exhibition held in Houston, Texas, 3-6 October 1999.

This paper was selected for presentation by an SPE Program Committee following review of information contained in an abstract submitted by the author(s). Contents of the paper, as presented, have not been reviewed by the Society of Petroleum Engineers and are subject to correction by the author(s). The material, as presented, does not necessarily reflect any position of the Society of Petroleum Engineers, its officers, or members. Papers presented at SPE meetings are subject to publication review by Editorial Committees of the Society of Petroleum Engineers. Electronic reproduction, distribution, or storage of any part of this paper for commercial purposes without the written consent of the Society of Petroleum Engineers is prohibited. Permission to reproduce in print is restricted to an abstract of not more than 300 words; illustrations may not be copied. The abstract must contain conspicuous acknowledgment of where and by whom the paper was presented. Write Librarian, SPE, P.O. Box 833836, Richardson, TX 75083-3836, U.S.A., fax 01-972-952-9435.

Abstract

Using electrical conductivity as a parameter to characterise the curing of cement slurries show promising results.

The paper describes how to measure conductivity, including practical observations and gained experience. We found that conductivity as a function of time for each slurry exhibits a characteristic curve form which clearly shows the curing behaviour. A relationship between conductivity and compressive strength was obtained and it was confirmed that rapid curing will reduce the risk of gas migration. Some observations on curing vs. additives are presented as well.

Measuring electrical conductivity is easy, and as such, could be used in the laboratory as a supplement to the equipment recommended by API, or in the field as a quality control during cementing operations.

Introduction

Cementing is an essential operation during construction of an oil or gas well. The quality of the cement behind a casing plays a vital role during drilling of the next interval, the production period of the well, and has a serious impact on the secondary cementing, workover and stimulation operations.

There is a large number of factors affecting curing and quality of cement. To achieve good zonal isolation the slurry should be tested and characterized by relevant parameters. Some of the cement material parameters and the procedures for testing them are described in the API specifications,¹ which include rheology, gel strength, free water, stability, initial setting, consistency and other. Unfortunately the API specifications do not cover every issue, especially regarding gas migra-

tion or continuous monitoring of the cement curing. Another problem is the discrete character of the measurements, i.e. they describe the slurry at preselected time points, while the cement slurry properties change continuously due to the hydration process for a long period of time. These facts are important in analysing the behaviour of the cement after a cementing operation. The present paper describes a method for continuous monitoring of cement curing.

The work presented in this paper was part of a larger project carried out to investigate gas migration and early time hydration of oil well cement. Other investigated parameters included temperature evolution, hydrostatic pressure, tensile strength, permeability, and shrinkage.² Electrical conductivity (the inverse of resistivity) was a candidate for investigation because it depends on porosity and the ions in the pore fluid. During hydration of cement, a cement matrix structure is build up at the same time as the porosity is reduced, which should manifest itself as a characteristic continuous conductivity decline. The level and shape of the curve would therefore give valuable information on the setting process. It is widely recognized that the risk of gas migration is reduced with a short transition period which should easily be seen from the conductivity curves. Furthermore, as gas cannot conduct electricity, gas flowing through the cement should lead to a relatively abrupt conductivity decline. This could be used to detect and track gas as it migrates upwards a cement column.

No work has been presented on oil well cement and conductivity, but a fair amount of literature exists on conductivity vs. concrete and other cement applications. In addition to presenting their own results, Christensen *et al.*³ also include an extensive review of previous work; in the beginning, electrical conductivity was used for finding initial set and for following the rest of the hardening process. The method has also been used to estimate porosity of fresh concrete, influence of additives, and corrosion risk of concrete reinforcements. Comparison between conductivity and permeability has shown promising results, and other work show that conductivity may be related to cement microstructure.

One parameter that has not extensively been connected to conductivity, though, is strength build-up. Predicting strength from conductivity during cementing is valuable because the time until operations can be resumed could be estimated, reducing WOC, down-time and costs. Although not directly con-

*Now at University of Mining and Geology, Sofia, Bulgaria.

nected to cement, Ishchuk *et al.*⁴ have looked at conductivity and yield point of a lithium soap/oil system, and some further interpretation of their data show a good correlation. Rengaswamy *et al.*⁵ have investigated several concrete mixes from 1 to 28 days, with the same result; an almost linear correlation between compressive strength and conductivity. Ding *et al.*⁶ have also monitored both parameters.

This paper is a continuation of a previous paper.⁷ The previous paper mainly dealt with the theoretical aspects of cement and conductivity, whereas this paper covers the practical work, gained experience, and results.

Measurement Principle

This section is a short review of the principle of electrical conductivity measurements and some observations concerning the method and its applicability. For a more thorough discussion on cement and electrical conductivity in general, we refer to Christensen *et al.*,³ and in particular for oil well cement, to Backe *et al.*⁷

Electrical conductivity is the material property which describes the ability to carry electrical current through the material. The measurement principle is shown in the left hand of **Fig. 1** where alternating current (AC) is sent through the cement via two metal electrodes which cover the whole end-sides of the cement sample. The conductivity (σ) is calculated from the current (I), voltage drop (U), and the geometry of the cement sample:

$$\sigma = G \frac{I}{U} \dots\dots\dots (1)$$

The constant G is a geometrical factor which has to be determined experimentally for each setup using an electrolyte with known conductivity.

Several tests were done to find out more about the applicability of the method. The first was to assure that there is no negative effect from the current on the cement curing. This was done by running two parallel tests, one with and one without conductivity measurement, and using temperature evolution as a quality control. As shown in **Fig. 2**, there is no adverse effect from the current going through the cement. The small temperature difference is caused by a small calibration difference between the two sensors. Another test at 90°C produced the same result.

Conductivity is highly sensitive to temperature, and in order to compare slurries at different temperatures, a correction has to be applied. In our study corrections have been done by using the Arps⁸ equation for normalising the conductivity to 25°C.

In some cases the 2 electrode setup to the left in **Fig. 1** may produce false readings because of the contact resistance between electrodes and testing material. This additional resistance introduces an extra artificial voltage drop which lead to errors. This problem can be avoided by using 4 electrodes as shown in the right hand of **Fig. 1**, two for current and two for measuring the voltage drop. To find out if this was a problem

for cement, both 2 and 4 electrodes have been used simultaneously in the same test. Results from a test are shown in **Fig. 3**. The curves agree well. The small fluctuation in the first 2 hours is probably caused by uneven temperature distribution within the cement. Both electrode configurations have been used in our work.

Some tests were run with a water layer on top of the cement slurry to see how surrounding formation water would influence conductivity. The additional water led a higher conductivity at a later stage compared to those tests without a water layer (see **Fig. 4**). This difference is explained by cement shrinkage: During hydration the cement will shrink, and this shrinkage will be compensated for with whatever fluid that is around the cement. Water conduct current whereas gas will create voids that lowers the conductivity. To make the tests comparable, all tests presented in this paper have been run without a water layer.

Measurement Setup

The practical measurements in the study included several different cells. Initially some very simple cells made from plastic coated cardboard boxes were used to verify that electrical conductivity could be used on cement. These tests were successful and subsequently several other cells were used as described below.

Minigasrig. As mentioned above, this work was carried out to investigate gas migration and early time cement hydration. Initially a PVC version of the minigasrig was used at ambient conditions to verify the concept. The principle of the cell with a gas inlet at the bottom and an outlet at the top is shown in **Fig. 5**. A differential pressure was applied between them to simulate the driving force behind gas migration; the chosen pressure was higher than the hydrostatic pressure of a water column, but smaller than the cement hydrostatic pressure. Several electrode pairs were placed along the cell to detect and track the gas migration front and metal endplates served as current electrodes.

These initial tests were successful and consequently a cell based on the same concept was designed to study gas migration at high temperature and high pressure (HTHP). This version can be used at temperatures up 180°C and pressures up to 20 bars. The HTHP cell has a 5 cm inner diameter and a height up to 80 cm. The cell is modular consisting of several sections that can be stacked on top of each other (see **Fig. 6**). Depending on the preferred test conditions, the cell can be used with a different number of sections. The sections were electrically insulated by Viton rubber sleeves and connected together with Teflon rings which carried the electrodes. Usage of rubber sleeves enabled applying confining pressure to avoid microannulus between cement and wall. The rig was used successfully up to 140°C, but at 180°C some problems with the rubber sleeves were observed.

ECMIC. The “Electrical Conductivity Measurements In Cement” cell (ECMIC) is shown in **Figs. 7 and 8**. In this cell the current flows radially between the center electrode and the circumference of the cell. The center electrode includes a temperature sensor and the bottom of the cell is electrically insulated with a rubber mat. It has a diameter of 85 mm and the height is 50 mm. The cell was designed for pressures up to 20 bars and temperatures up to 200°C. Some contact problems were experienced between the outer wall and the cement caused by cement shrinkage. This problem was solved by attaching a brass foil along the outer circumference. This was successful but increased the preparation time somewhat.

Glass test tube. Ever in the search for better solutions, a disposable cell in the form of a glass test tube was introduced. The principle is shown in **Fig. 9**. The outer diameter is 30 mm and the height is 200 mm. High temperature silicone insulated wire was used, with the non-insulated ends serving as electrodes, making this a 2 electrode setup. The test tube was placed inside a HTHP consistometer (the type without a magnetic coupling at the top) increasing the pressure range significantly. One drawback is the lower temperature evolution inside the cement, because both the cement volume and test tube diameter are smaller than for the cells above. Another drawback is that the chosen disposable temperature sensors do not withstand temperatures above around 150°C.

Results and Discussion

The test program comprised around 40 tests using both neat cement mixes and commercial cement slurries. The mixing procedure was according to the recommendation of API.¹ In this section some of our results and observations are presented and discussed.

Consistency. A magnetic stirrer has been used together with the Ecmic cell (Fig. 6) as a consistency measurement. The stirrer was placed underneath the cell and a magnetic stirring pin (50×7.5 mm) was placed inside. As the power of the electric motor is more or less constant, the RPM will decrease when the cement is thickening. The RPM was measured manually by a handheld tachometer. Results from an experiment at 140°C is shown in **Fig. 10** which clearly shows the start of thickening. The increasing RPM up to 1.5 hours is probably caused by heating leading to a lower cement viscosity. It also worth noting that thickening occurs before the hydration starts, as indicated by temperature and conductivity curves.

Additives. No detailed investigation on additives were carried out, but several findings can be seen in the results. A representative selection covering the temperature range from ambient conditions and up to 195°C are presented in **Figs. 11 to 19** where the slurries are shown in order of increasing temperature. All slurries, except the first (Fig. 11), are commercial recipes.

One of the most interesting observations can be found in Fig. 16 which investigated the influence of manganese oxide and silica fume on curing of a 150°C slurry.⁹ The manganese oxide is used as weight material and the silica fume as an anti gas migration additive where the minute silica particles fill the pore space between the cement grains. The first test was run with both additives, then followed by in turn removing one additive at a time. Both additives were removed in the last test. From the figure it is evident that silica fume has a dramatic impact on the curing behaviour, reducing the time between initial and final set to almost nothing. Another experiment at 140°C exhibited the same behaviour. A short transition period will reduce the risk of gas migration. This is shown later.

When used together with silica fume, it seems that the weight material acts as an accelerator (see Fig. 16). The main difference between the two slurries in Fig. 14, apart from the small temperature difference, is that the 142°C slurry includes manganese oxide and almost twice as much retarder as the 136°C slurry which do not have any weight material. The amounts of retarder and the small temperature difference cannot fully explain that the setting behaviour of the two slurries are almost identical, again indicating that manganese oxide counteracts the increased amount of retarder in the 142°C slurry, i.e., it acts as an accelerator.

Fig. 13 shows the impact of low and medium temperature retarders on two 136°C slurries. The clear difference is worth noting bearing in mind that a short transition time is beneficial for impeding gas migration. None of the two slurries in Fig. 15 contain silica fume, but the silica flour was replaced by calcite flour (CaCO₃) in the second test. Like silica fume, calcite seems to cause rapid curing.

Of course retarders and other additives influence the curing behaviour to a large extent, but looking at Figs. 11 to 19 we feel that some of the behaviour may be attributed to temperature. When using silica fume (all slurries except Figs. 11, 15, and partly 16), there seems to be a very rapid curing at 140-150°C, whereas at 165°C (Fig. 17) the hardening is slow. Increasing the temperature further seems to accelerate curing, producing faster curing at 180°C (fig. 18) and even faster again at 195°C (Fig. 19).

The results and observations above build on a limited set of tests and they should be verified by a systematic investigation of additives over the temperature range. However, our findings so far underline the valuable data gathered from electrical conductivity curves.

And as an anecdotal aside, some slurries exhibit two temperature peaks (e.g. in Fig. 18 at around 7 and 12 hours) and others only one. These were nicknamed camel- and dromedary-slurries, respectively.

Gas migration. The minigasrig was used to investigate gas migration in the early setting period of the cement slurry. A result from a neat slurry test at ambient conditions in the PVC cell is shown in **Fig. 20** where the gas front is clearly seen as it

migrates upwards through the cement column. Electrode pair 1 is lowermost while 5 is at the top. Some high temperature commercial slurries were tested as well and all proved to be tight. This corresponds to the results from the larger gas rig of Jamth *et al.*^{10,11} using the same slurry recipes.

The conductivity data were compared to gas migration tests run in the rig of Jamth *et al.*^{10,11} The results are shown in **Fig. 21** where the conductivity is normalised to the conductivity level just before the hydration starts (e.g. at 8-9 hours in **Fig. 12**). This is done in order to be able to compare slurries with different initial conductivities. It was found that the maximum normalised decline rate exhibited a good correlation, except that there seems to be an anomaly for 90°C slurries; a high decline rate, i.e. a short transition period, will reduce the likelihood for gas migration.

Compressive strength. There is not much literature on electrical conductivity and cement strength. Although not directly connected to cement, Ishchuk *et al.*⁴ have investigated the conductivity and yield point of lithium soap/oil systems. Interpretation of their data in **Fig. 22** show a clear correlation between strength and conductivity. The data of Rengaswamy *et al.*⁵ are more relevant, covering concrete between 1 and 28 days. Their results in **Fig. 23** show an excellent correlation between compressive strength and resistivity (the inverse of conductivity). Comparison of the 12 and 24 hour data of Ding *et al.*⁶ also reveal a correlation (see **Fig. 24**).

We have not carried out any direct comparison between the two parameters, but we have correlated compressive strength from the ultrasonic cement analyzer (UCA) to conductivity data. In the comparison it is assumed that the cement exhibit no strength before the normalised conductivity reaches 0.6. Normalisation was done for the same reason as above. The results are shown in **Fig. 25** where there are some spread among the curves. Part of this spread may be explained by the UCA strength which itself is an estimate. Nevertheless, we can estimate when the drillout criterion¹² is reached and operations can resume, i.e., when the normalised conductivity reaches 0.2. For comparison, slurry no. 4 reached the drillout criterion at 4 hours, whereas the four others were around 10-12 hours.

Conclusions

1. Electrical conductivity is a simple and reliable method to track the hydration process of a cement slurry. Tests has been carried out to assure the applicability of the method.
2. Each slurry exhibits a characteristic continuous conductivity decline. The level and shape of each curve gives valuable information on the setting process. A short transition period, which is important for avoiding gas migration, is easily seen.
3. Some interesting observations were found concerning additives. The most important is that silica fume was found to reduce the transition period significantly.
4. A correlation was found between conductivity and compressive strength, and between conductivity and gas migra-

tion: the risk of gas migration is reduced with a rapidly setting slurry.

5. Based on these findings, we feel that electrical conductivity has the potential to be used in the laboratory as a supplement to the equipment recommended by API as well as in the field to control the slurry quality during cementing.

Nomenclature

G = geometric constant, 1/L, 1/m

I = electric current, q/t, A

U = electric potential difference, mL²/qt², V

σ = electrical conductivity, tq²/mL³, S/m

References

1. *Spec. 10, Specification for Materials and Testing for Well Cements*, fifth edition, API, Dallas (1990).
2. Backe, K.R., Lile, O.B., Lyomov, S.K., Elvebakk, H., and Skalle, P.: "Characterising curing cement slurries by permeability, tensile strength, and shrinkage," paper SPE 38267 presented at the 1997 SPE Western Regional Meeting, Long Beach, California, 25-27 June.
3. Christensen, B.J., Coverdale, R.T., Olson, R.A., Ford, S.J., Garboczi, E.J., Jennings, H.M, and Mason, T.O.: "Impedance Spectroscopy of Hydrating Cement-Based Materials: Measurement, Interpretation, and Application," *J. of the American Ceramic Society* (November 1994) **77**, No. 11, 2789.
4. Ishchuk, Yu.L., Podlennykh, L.V., and Godun, B.A.: "Effect of temperature on structure and properties of lithium soap/oil systems," *Chemistry and Technology of Fuels and Oils* (September 1989) **25**, No. 1-2, 53.
5. Rengaswamy, N.S., Srinivasan, S., Mahadeva Iyer, Y., and Suresh Babu, R.H.: "Non-destructive testing of concrete by electrical resistivity measurements," *Indian Concrete J.* (January 1986) **60**, No. 1, 23.
6. Ding, X.Z., Zhang, X., Ong, C.K., Tan, B.T.G., and Yang, J.: "Study of Dielectric and Electrical Properties of Mortar in the Early Hydration Period at Microwave Frequencies," *J. of Materials Science* (October 15, 1996) **31**, No. 20, 5339.
7. Backe, K.R., Lile, O.B., and Lyomov, S.K.: "Characterising Curing Cement Slurries by Electrical Conductivity," paper SPE 46216 presented at the 1998 SPE Western Regional Meeting, Bakersfield, California, 10-13 May.
8. Arps, J.J.: "The Effect of Temperature on the Density and Electrical Resistivity of Sodium Chloride Solutions," *Trans., AIME* (1953) **198**, 327.
9. Justnes, H., Backe, K.R., and Jamth, J.: "Gas Tight Slurries for Oil Well Cementing at High Temperature and Pressure (HTHP) Conditions," report no. STF22 F96804.35, SINTEF Civil and Environmental Engineering, Trondheim, Norway (1996).
10. Jamth, J., Justnes, H., Lile, O.B., Nødland, N.E., Skalle, P., and Sveen, J.: "Large scale testing system to evaluate the resistance of cement slurries to gas migration during hydration," paper 95-405 presented at the 1995 CADE/CAODC Spring Drilling Conference, Calgary, April 19-21.
11. Jamth, J.: "Apparatus and a Method for the Testing of Concrete for Use When Cementing Casings in Oil and Gas Wells," U.S. Patent No. 5,571,951 (1996).
12. Rae, P.: "Cement Job Design," *Well Cementing*, E.B. Nelson (ed.), Schlumberger Educational Services, Houston (1990) Chap. 11.

SI Metric Conversion Factors

$^{\circ}\text{F} (^{\circ}\text{F}-32)/1.8$	$= ^{\circ}\text{C}$
$\text{ft} \times 3.048^*$	$\text{E}-01 = \text{m}$
$\text{in.} \times 2.54^*$	$\text{E}+00 = \text{cm}$
$\text{lb}/100\text{ft}^2 \times 4.788\ 026$	$\text{E}-01 = \text{Pa}$
$\text{mL} \times 1.0^*$	$\text{E}+00 = \text{cm}^3$
$\text{psi} \times 6.894\ 757$	$\text{E}-02 = \text{bar}$
$\text{psi} \times 6.894\ 757$	$\text{E}-03 = \text{MPa}$
$\text{U.S. gal} \times 3.785\ 412$	$\text{E}-03 = \text{m}^3$

*Conversion factor is exact.

Acknowledgements

The authors would like to thank the sponsors of this work: Norsk Hydro, The Research Council of Norway, Saga Petroleum, and Statoil. We also thank Pål Skalle, Harald Elvebakk, Jostein Sveen, Harald Justnes, and John Jamth for valuable discussions.

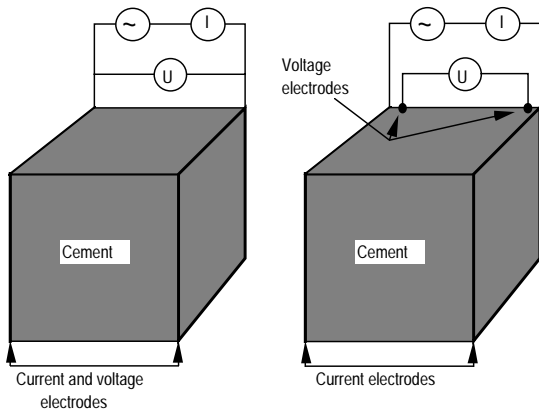


Fig. 1—Measurement principle of electrical conductivity. Two-electrode setup to the left, and to the right four-electrode.

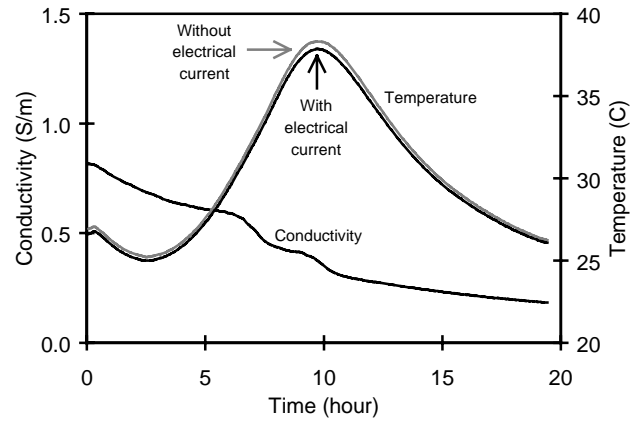


Fig. 2—Temperature evolution with and without conductivity measurement.

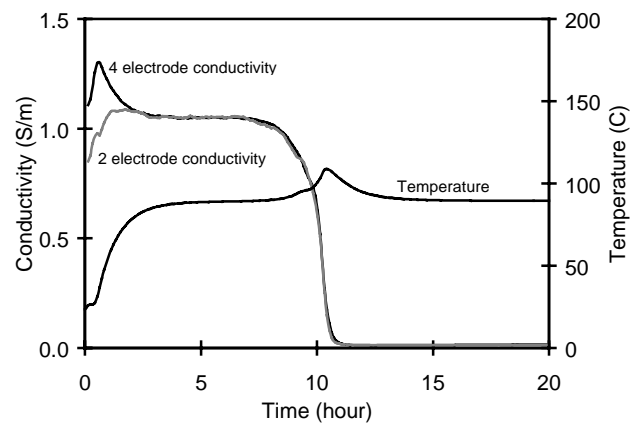


Fig. 3—Conductivity curves for a 90°C slurry using 2 and 4 electrodes.

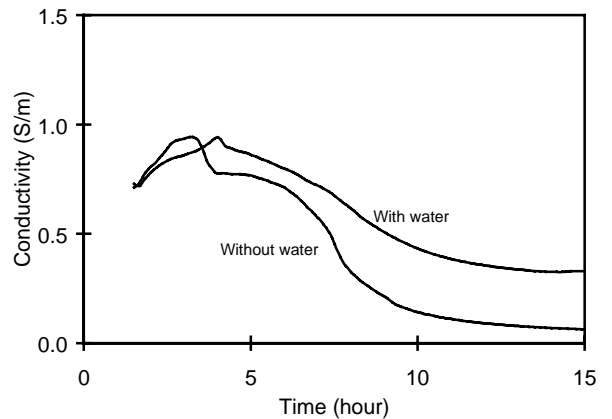


Fig. 4—Conductivity behaviour with and without water on top of the cement.

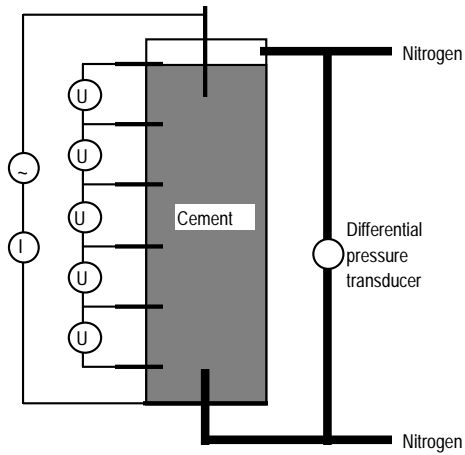


Fig. 5—Principle drawing of the minigasrig.

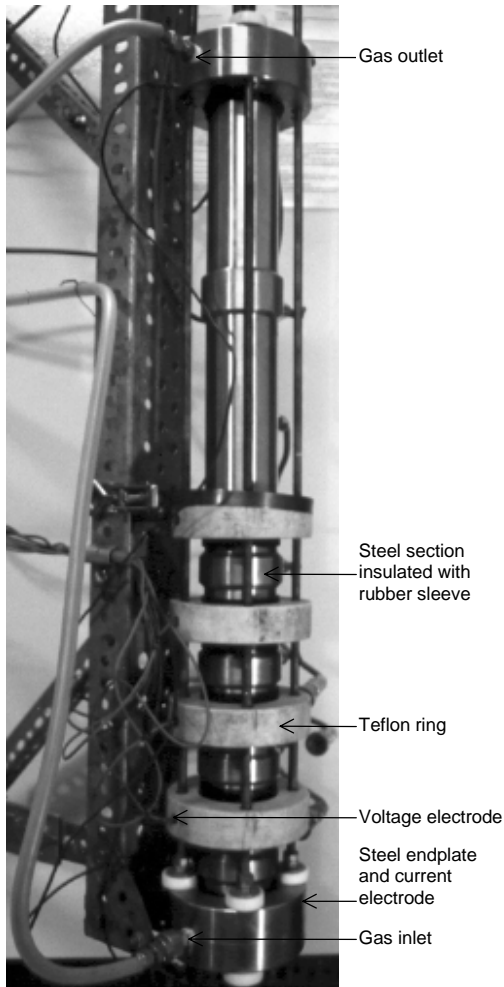


Fig. 6—Photograph of the HTHP minigasrig.

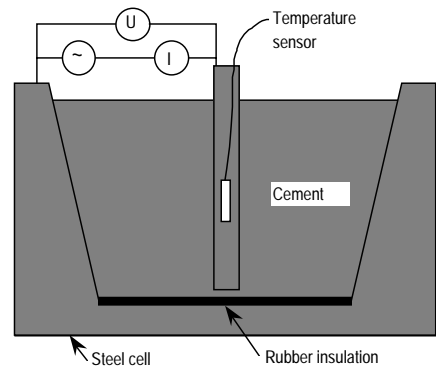


Fig. 7—Principle drawing of the Ecmic cell.



Fig. 8—Photograph of the Ecmic cell.

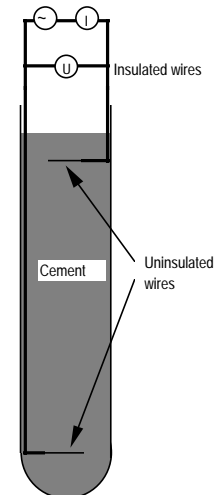


Fig. 9—Principle drawing of the glass test tube used in a HTHP consistometer.

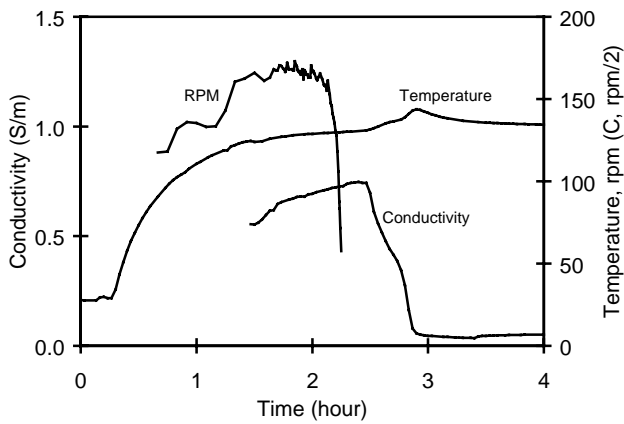


Fig. 10—RPM as a function of time using a magnetic stirrer in a 140°C slurry. This test was run in the Ecmic cell.

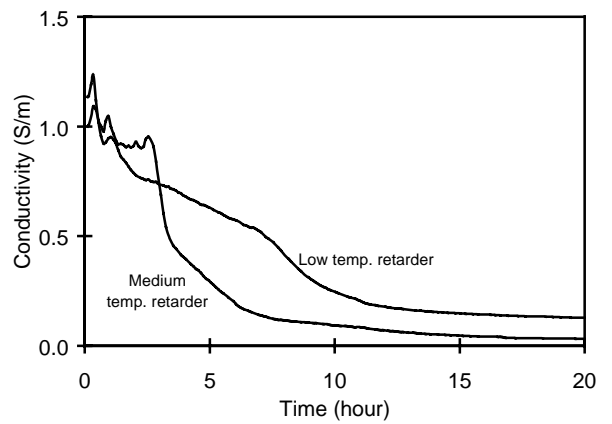


Fig. 13—Two tests at 136°C where the main difference is the use of low and medium temperature retarder. These tests were run using glass test tubes in a HTHP consistometer.

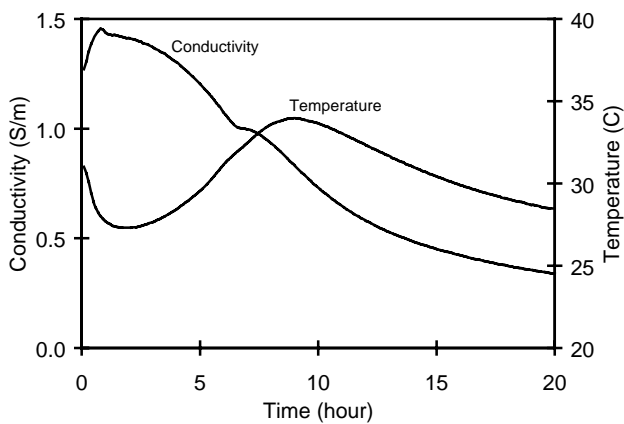


Fig. 11—A 0.5 w/c neat slurry at ambient conditions. This test was run in the minigasrig.

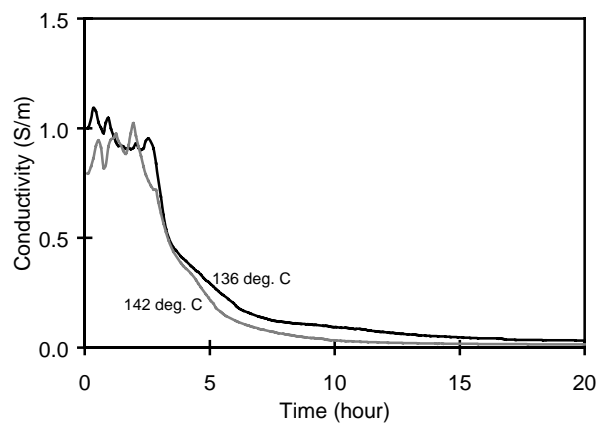


Fig. 14—Two tests at 136 and 142°C. The 136°C slurry has a low amount of retarder and no weight material (manganese oxide). The 142°C slurry has weight material and a higher amount of retarder. These tests were run using glass test tubes in a HTHP consistometer.

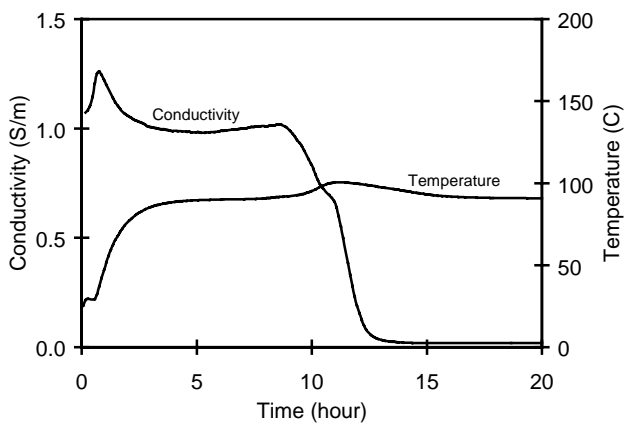


Fig. 12—Conductivity and temperature behaviour of a 90°C slurry. This test was run in the Ecmic cell.

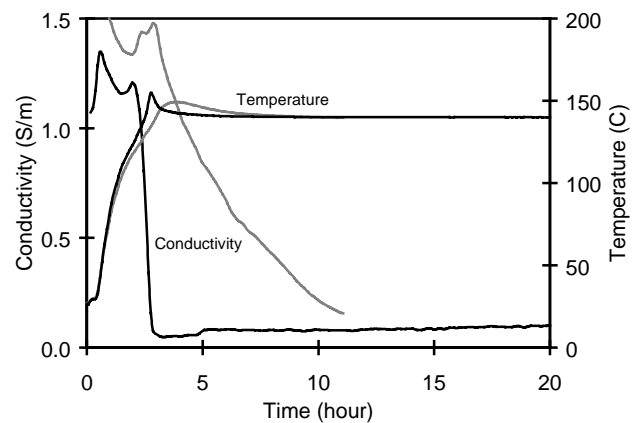


Fig. 15—Two 140°C slurries, one with silica flour (grey) and the other where the silica was replaced by calcite flour (black). These tests were run in the Ecmic cell.

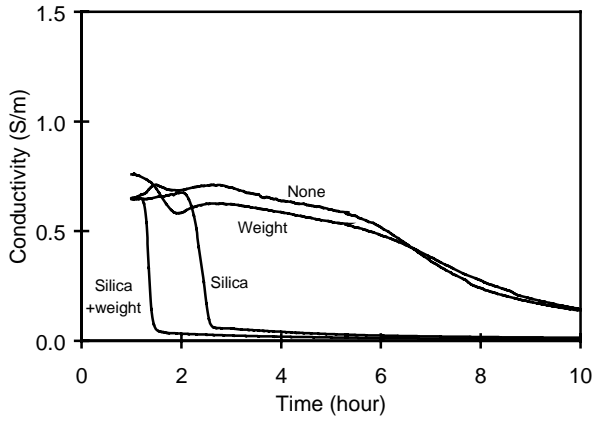


Fig. 16—Conductivity of a 150°C slurry when silica fume (“silica”) and weight material (manganese oxide, “weight”) were removed from the recipe. These tests were run using glass test tubes in a HTHP consistometer.

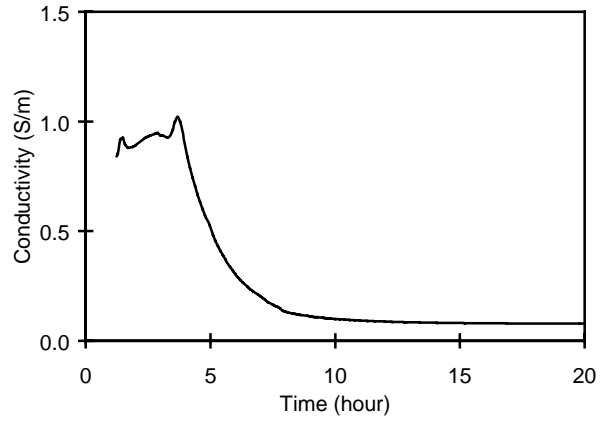


Fig. 19—Conductivity evolution of a 195°C slurry. This test was run using a glass test tube in a HTHP consistometer.

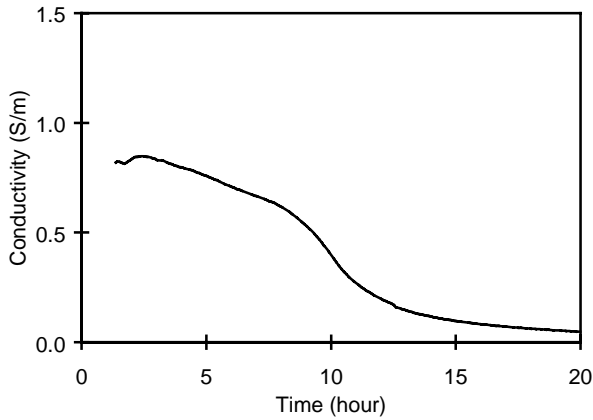


Fig. 17—Conductivity behaviour of a 165°C slurry. This test was run using a glass test tube in a HTHP consistometer.

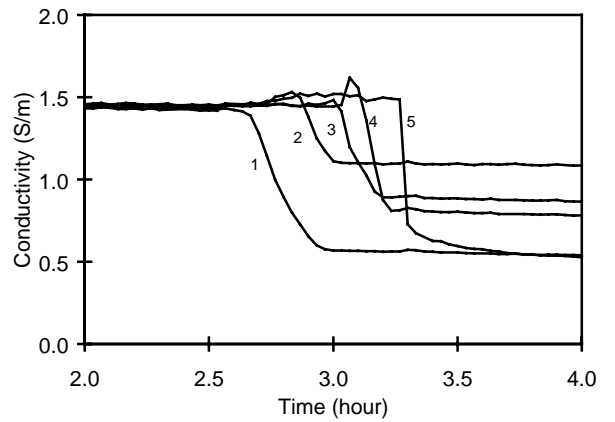


Fig. 20—Tracking of gas front in the minigasrig.

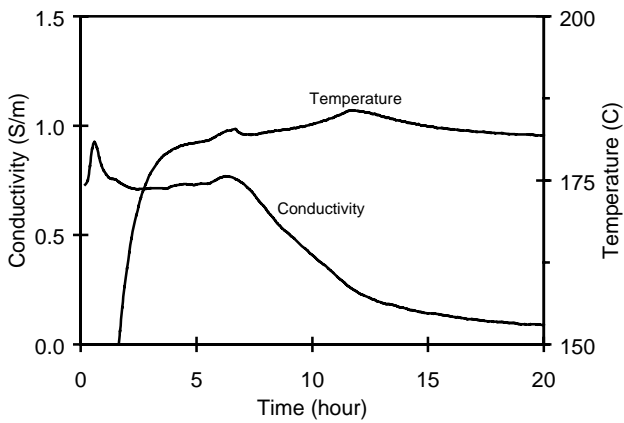


Fig. 18—Conductivity and temperature evolution of a 180°C slurry. This test was run in the Ecmic cell.

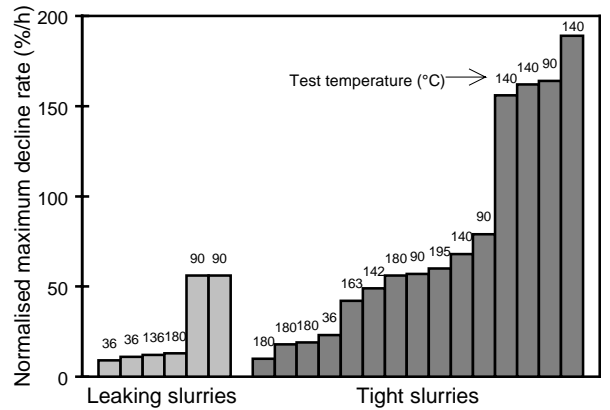


Fig. 21—Normalised maximum conductivity decline rate vs. gas tight and leaking slurries.

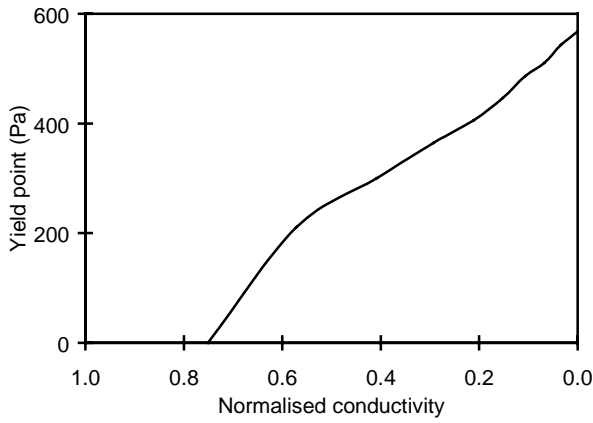


Fig. 22—Strength vs. conductivity for a lithium soap/oil system. Interpreted data from Ishchuk *et al.*⁴

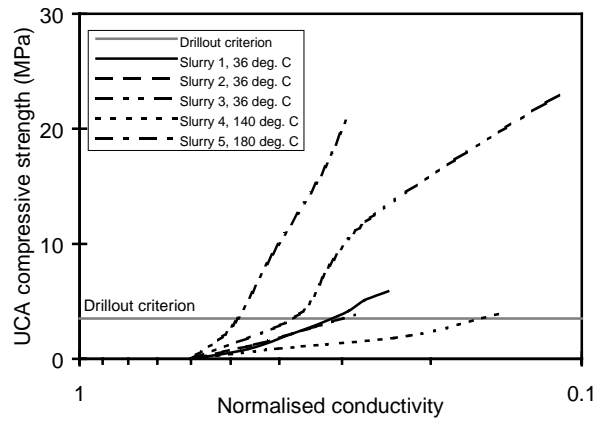


Fig. 25—Correlation between UCA compressive strength and normalised conductivity. It is assumed that the cement exhibit no strength before the normalised conductivity reaches 0.6.

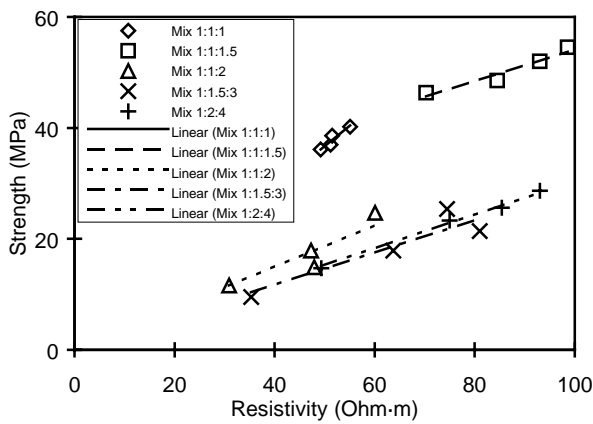


Fig. 23—Strength vs. resistivity for five concretes from 1 to 28 days. All line fits, except the mix 1:1:1.5 (cement:sand:aggregate), go through zero. Data from Rengaswamy *et al.*⁵

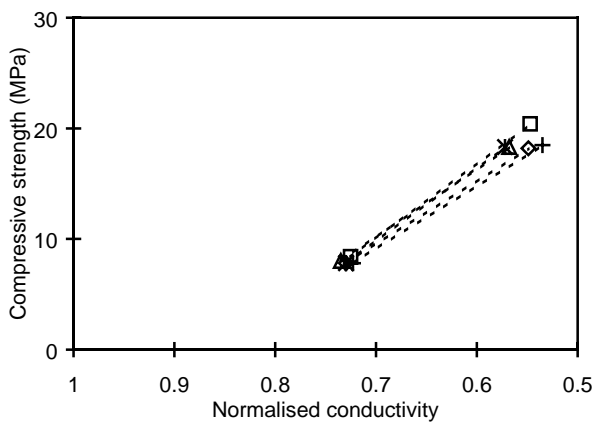


Fig. 24—Strength vs. conductivity for different sand/cement ratios. 12 and 24 hours data from Ding *et al.*⁶